Studying parameters for changing the initial particle arrangements of distinct element analysis in earthquake response based on slope analysis

Taiki Yoshida, Masato Nakajima, and Hitoshi Tochigi
Central Research Institute of Electric Power Industry, Abiko, Japan

Abstract: The Distinct Element Method (DEM) has been applied to analyze the earthquake response of slopes surrounding a nuclear power plant. Distinct element (DE) analysis includes uncertainty factors such as initial particle arrangement. A particularly difficult problem includes the question of how to determinate initial particle arrangement correctly; evaluating the inherent anisotropy of the actual surrounding slope or using actual anisotropy in the analysis model is unrealistic due to the size of the actual slope. However, if there are statistical patterns in the structure of the graphs of coarse-grained models in DE analysis, we may be able to use them for a highly developed Probabilistic Risk Assessment (PRA). This study was conducted to investigate the applicability of DE analysis to a shaking table model test and study the statistical patterns of results from 50 initial graph structures of granular materials. The probability distribution of failure timing was normally distributed and one of failure regions showed log-normal distribution in the numerical analysis. Their modes and means were close to experimental results. The next step would be to study the probability distribution of impact force needed to create a highly developed PRA using the Extended DEM.
Keywords: probabilistic risk assessment, Distinct Element Method, initial particle arrangements

1. INTRODUCTION

After the Great East Japan Earthquake, the level of the design for earthquake ground motion for nuclear power plants has been increased. Therefore, quantitative assessments of the seismic resistance of critical facilities, such as nuclear power plants, to earthquake-induced failure of surrounding slopes are becoming increasingly important as the deterministic approach in regulation. Further, evaluation of other aspects besides the design basis earthquake ground motion in probabilistic risk assessment (PRA) is important as the voluntary activity by corporation. Slopes failure around the nuclear power plant should be considered as events that accompany earthquakes in PRA.

A seismic risk assessment flowchart for rock slopes (Figure 1) was proposed by the Central Research Institute of Electric Power Industry (CRIEPI) [1]. The seismic risk assessment involves two steps given that there are earthquake ground motions consistent with target exceedance probability and hazard curve. In the first step, the sliding failure probability is calculated. In the second step, if structures near the slope may be critically affected by falling rock, the effects of falling rocks on nearby structures are quantitatively evaluated even if the frequency of this is low.

The seismic stability of the surrounding slopes is often represented by a safety factor (SF). This factor is defined as the ratio of resistance force derived from rock strength to the transient driving force due to an earthquake. It can be calculated by performing an equivalent linear analysis. However, even if the SF is less than one, the slope may not necessarily failure. Further, a rational evaluation of seismic stability may not be possible due to the excessive conservative margin of the equivalent linear analysis results. Therefore, evaluating seismic stability on the basis of ground displacement is a more rational approach. The CRIEPI recommends a time history nonlinear analysis for evaluating the stability of slopes, including post-earthquake residual displacement, and predicting a failure range when large deformations and displacements occur [2].

For the evaluation of the displacement of rock masses failed in the second step, the distinct element method (DEM) is often used. This is a discontinuous analysis method [3] and can evaluate large deformations or failures easily compared to the finite element method (FEM).

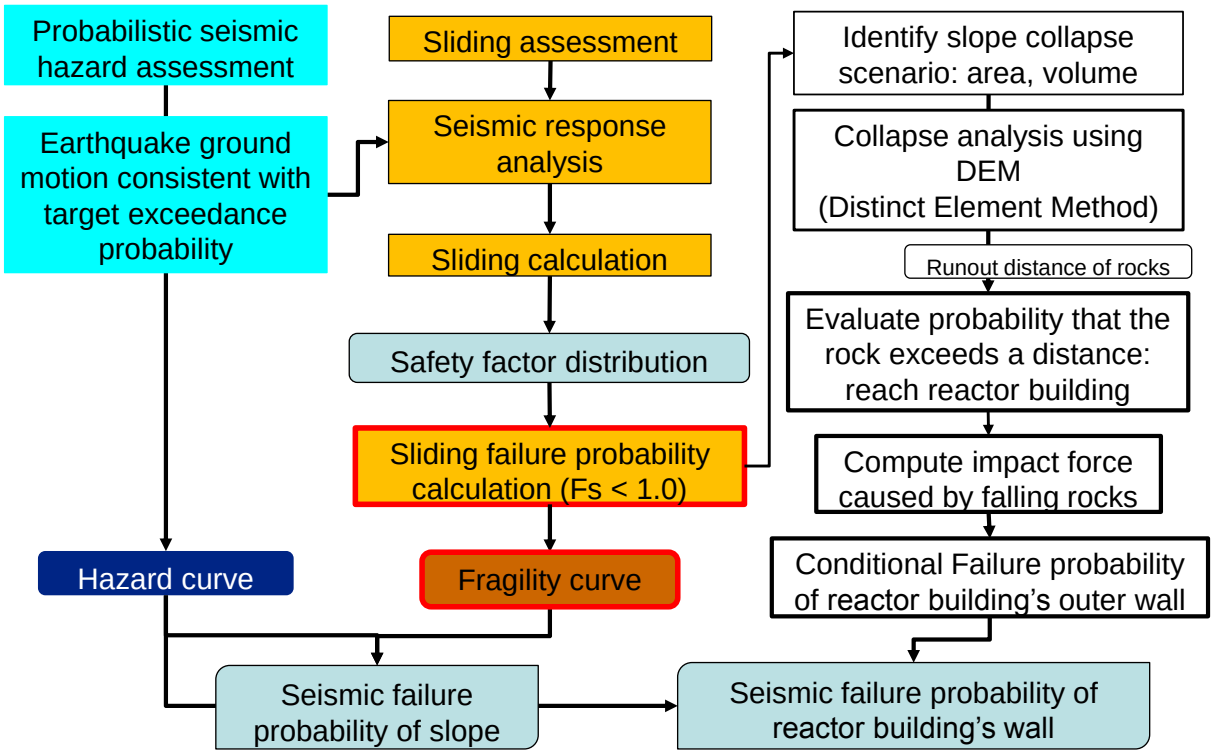

Figure 1. Seismic risk assessment flowchart for rock slopes [1]

The probability of a particle reaching at a particular distance was evaluated using the DEM by the CRIEPI [4]. Tochigi et al. determined it under gravity after they temporarily created a slip line using seismic intensity method.

However, some of these methods do not yield consistent results for the two steps. Further, the excessive conservative margin of the results cannot be avoided because consistent analysis results cannot be avoided. For example, in the DEM, particles are assumed to slip easily, and therefore the friction coefficient or residual strength is set at zero in the second step. In such a case, a rational evaluation may not be possible because of the excessive conservative margin.

Therefore, the earthquake response analysis of slope can be improved by including the transition from continuum to dis-continuum of slope seamlessly.

The Extended distinct element method (EDEM) may be effective for developing such a seamless analytical approach [5]. In the EDEM, a pore spring exists among the soil pores for cohesion between particles. By setting tensile strength and shear strength and turning off the pore spring if the pore force exceed their strength, the progressive failure of slopes can be modelled.

DE-analysis involves uncertainty factors such as spring coefficient, viscous damping coefficient, rolling friction coefficient, and initial particle arrangement. The initial particle arrangement affects the analysis results; however, determining this parameter correctly is particularly difficult [6]. Further it may indicate the inherent anisotropy; however, evaluating the initial structural anisotropy of the actual surrounding slope and using this information in the analysis model is an unrealistic approach because such a slope is so large that it costs too much to use the actual anisotropy in the analysis. The statistical patterns in the graph structure of the coarse-grained model in DE-analysis, can be used for PRA. Moreover, the variations in DE-analysis results with variations in initial particle arrangement should be investigated.

Some previous studies have investigated initial particle arrangements. In a previous study, we investigated the effect of initial particle arrangement in numerical simulations of an inclining model using the EDEM [7]. The probability distribution of the inclination angle was similar to the normal distribution when a slope failures and most of the slip lines defined in the analysis were near the slip lines in the experiment. Yoshida et al. investigated the influence of initial particle arrangement using the moving particle simulation (MPS) [8].

Such studies on initial particle arrangement are limited. However, the few studies that have been conducted demonstrate that the statistical pattern of the effect of initial particle arrangement and useful dates for conducting PRA considering the uncertainty of initial particle arrangement can be identified. If the statistical pattern of the effect of the initial particle arrangement can be identified, the uncertainty of the initial particle arrangement can be determined.

In this study, the earthquake response of a slope was studied through DE-analysis and considering fifty initial particle arrangements. Further, the applicability of DE-analysis to a shaking table model test and the statistical pattern of failure timing and region were determined.

2. SHAKING TABLE MODEL TEST

The geo-materials used to construct the slope model were composed of stainless particles, iron sand, and water. They were mixed at a 40:30:1 ratio. The physical parameters were obtained from laboratory results of a plane strain compression test, cyclic tri-axial test, and uniaxial tension test, as presented in Table 1. σ is confining pressure in Table 1.

Table 1: The physical properties of geo-material

Physical property	Value
Wet unit weight [kg/m^3]	4.20×10^3
Poisson ratio [-]	9.00×10^{-2}
Static elastic modulus [MPa]	$1.36 \cdot \sigma^{1.03}$
Initial shear elastic modulus [MPa]	$34.44 \cdot \sigma^{0.32}$
Tensile strength [kPa]	0.5
Peak shear strength [kPa]	$7.0 + \sigma \cdot \tan40.9^\circ$
Residual shear strength [kPa]	$2.05 \cdot \sigma^{0.69}$

The scale of the slope model, which had a slope gradient of 1:0.5, is presented in Figure 2.

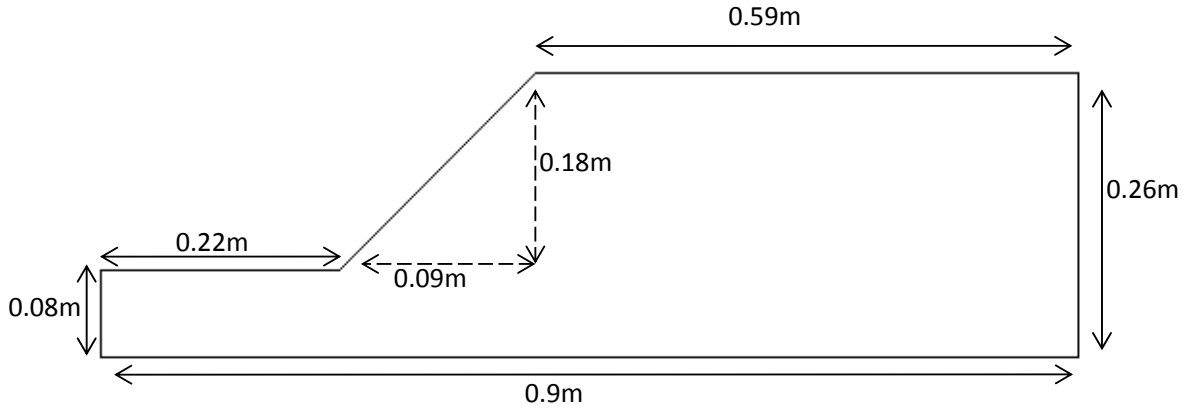

Figure 2. The scale of the slope model used in this study

The model was shaken in 16 stages at input accelerations. The input acceleration was a sinusoidal waveform, with the main section consisting of 20 waves at a frequency of 20 Hz. The horizontal acceleration waveforms measured at the bottom of soil bin in this test is shown as an example in Figure 3.

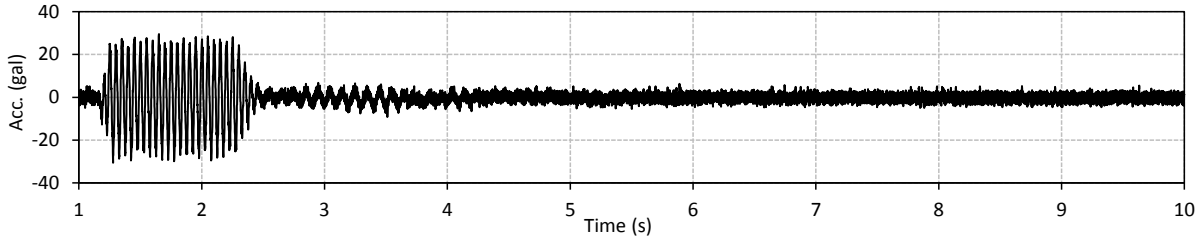

Figure 3. The horizontal acceleration measured at the bottom of the soil bin during the third stage of the shaking table model test

3. DISTINCT ELEMENT METHOD (DEM) FOR SOFT ROCK

For the numerical simulation, we used Itasca PFC3D code and constrained particles from moving out of the plane direction to model granular materials as a 2D analysis. When calculating the force between particles, there is a spring coefficient for contact force, a viscous damping coefficient for energy attenuation, a divider for ignoring tensile force, and a slider for dynamic friction force. Initial particle cohesion is modeled as a parallel bond, and the motion of each particle is expressed as follows:

$$\frac{d\boldsymbol{P}}{dt} = \sum \boldsymbol{F} \tag{1}$$

$$\frac{d\boldsymbol{L}}{dt} = \sum \boldsymbol{N} \tag{2}$$

where $\boldsymbol{P}$ represents linear momentum, $\boldsymbol{F}$ stands for the force acting on the soil element, $\boldsymbol{L}$ is angular momentum, and $\boldsymbol{N}$ is the torque acting on the soil element.

To classify material properties depending on confining pressure, we divided the slope model vertically into three layers as shown in Figure 4, where red area represents 1.78kPa, the blue expresses 5.35kPa and the green is 8.92kPa in terms of confining pressure.

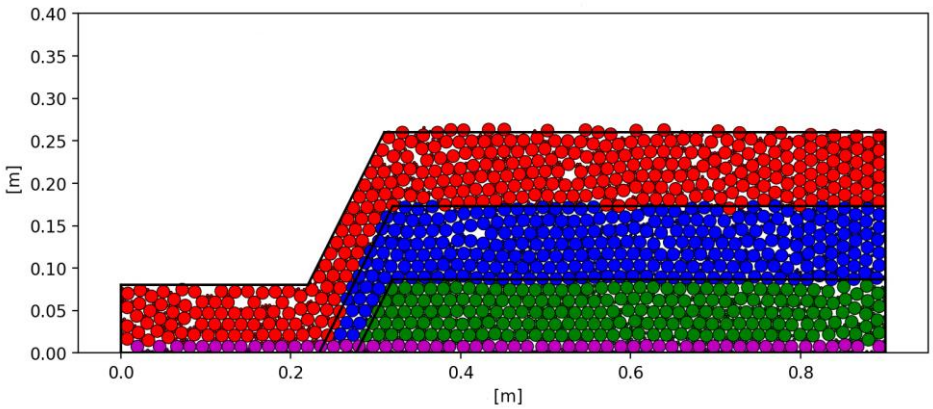

Figure 4. An example of the analytical model of slope

For the boundary condition, the front and the back were modeled as a rigid wall and the particles at the bottom of the soil bin, shown in purple in Figure 4, were fixed.

Fifty models of changing initial particle arrangements were prepared. Each model was composed of two kinds of particles whose diameters were 3mm and 15mm.

The DEM parameters for contact force are given in Table 2. The spring coefficient, pore spring coefficient, and shear strength are determined from the plane strain compression test while the dynamic friction coefficients was based on the cyclic tri-axial test. Tensile strength was based on the uniaxial tension test.

Table 2: DEM parameters for contact force

Layer number	First	Second	Third
Wet unit weight [kg/m^3]	4.20×10^3		
Normal spring coefficient [N/m]	4.25×10^7	5.51×10^7	6.51×10^7
Tangential spring coefficient [N/m]	1.92×10^7	2.48×10^7	2.93×10^7
Normal pore spring coefficient [N/m]	1.28×10^5	1.65×10^7	1.95×10^7
Tangential pore spring coefficient [N/m]	5.76×10^4	7.44×10^4	8.79×10^4
Normal damping ratio [%]	3		
Tangential damping ratio [%]	3		
Inter-particle friction angle [°]	34		

Inertial force was added to the center of the particles using horizontal acceleration waveforms measured at the bottom of soil bin in the shaking table model test. The shaking started from the third stage in the numerical simulation because there was white noise excitation and a low response from the slope in the first two stages.

4. RESULTS AND DISCUSSION

4.1. Experimental and Analytical results

During the experiment, the slope failed at stage 11; and after a lump of earth in the landslide was removed and the slip surface investigated, it was found that the top of slip line presented in Figure 5 was located at a point with a horizontal distance of 0.08 m from the top of the slope.
The histograms of the results of the numerical analysis are presented in Figure 6 and Figure 7. In this analysis, failure timing and region are defined by setting a threshold for particle displacement assumed in the following way: 1) excluding particles whose movements are more than threshold, considering them as falling, 2) defining the particle on the upper right of the remaining particles at the

left of the foot of slope as the lower left of slip line, 3) defining the particles on the upper left of the remaining particles at the right of the top of slope as the upper right of slip line, 4) determining that one of the particles at the slope surface and around the perpendicular bisector between the two points is the midpoint of slip line, and 5) defining the slip line as the one which passes its lower left, upper right, and midpoint. The resulting distribution of slope is shown in Figure 8 and 9.

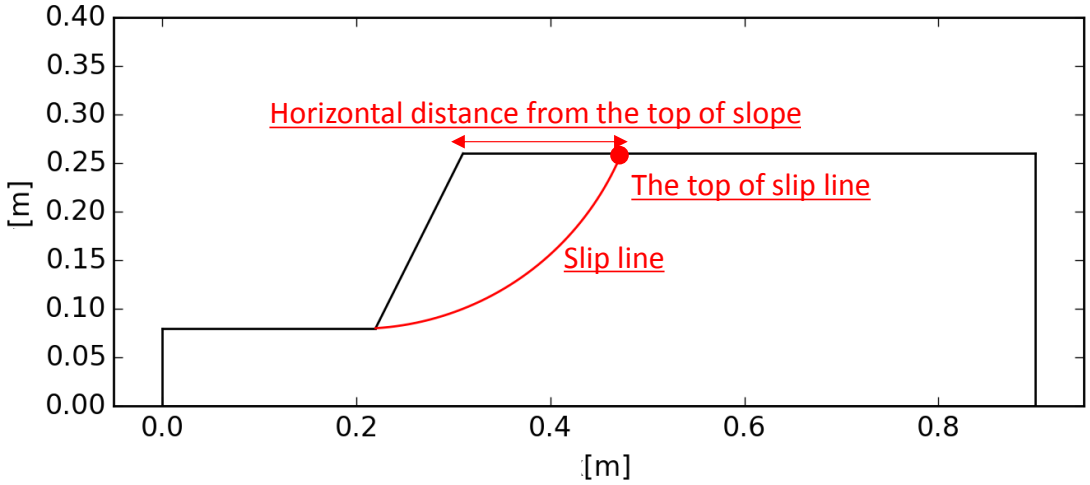

Figure 5. Concepts to analyze observed slip lines

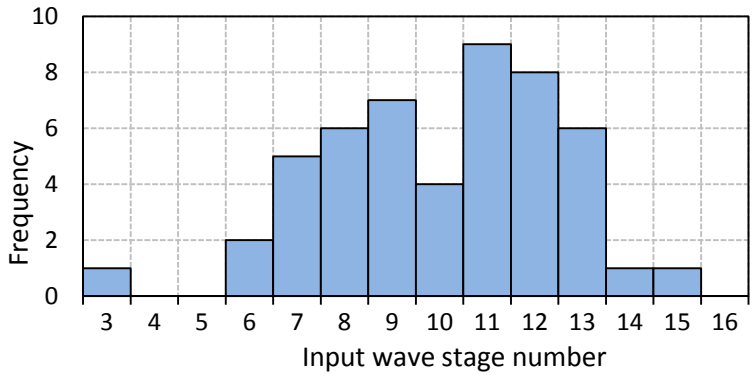

Figure 6. The failure timings from the numerical analysis

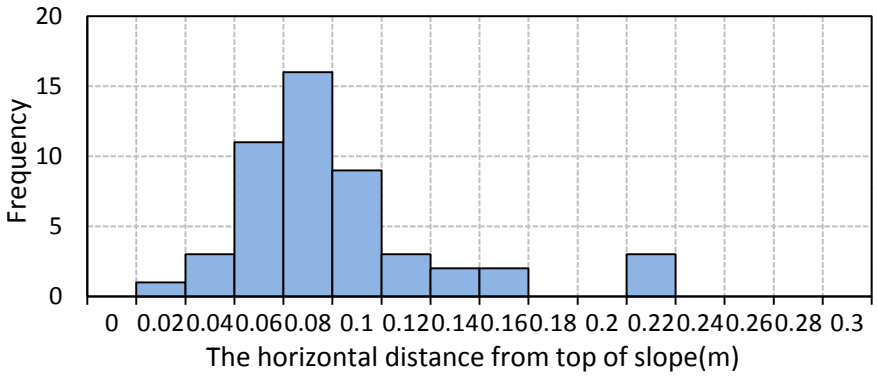

Figure 7. The location of the top of the slip line in the numerical analysis

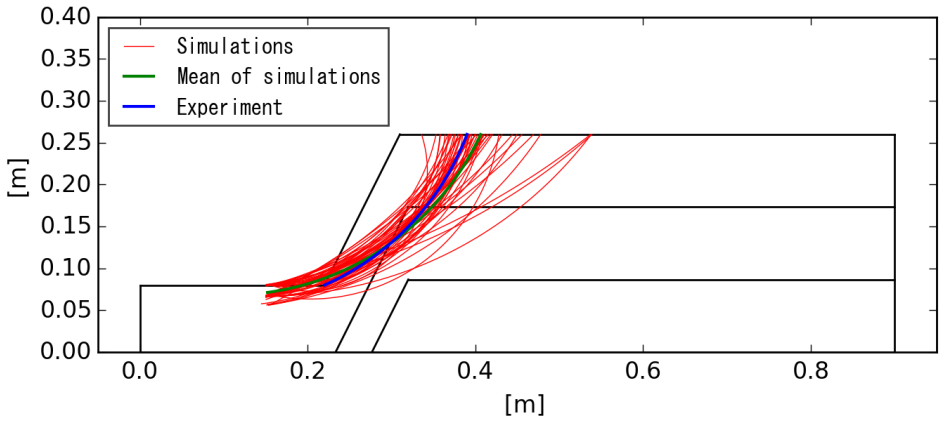

Figure 8. The distribution of the slip lines in the numerical analysis and the mean

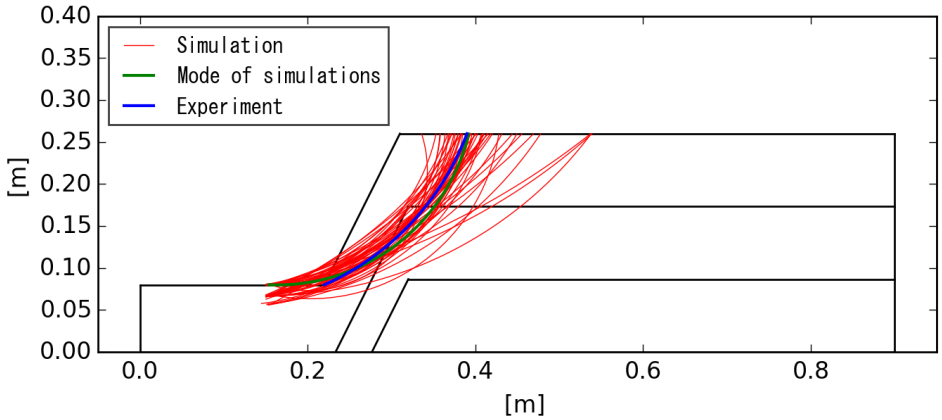

Figure 9. The distribution of the slip lines in the numerical analysis and the mode

The mean slip line of simulations in Figure 8 was defined as the line which passes the mean of each lower left point, upper right, and midpoint. The mean slip line was close to the experimental result. The mode slip line of simulations in Figure 9 was defined as the line which passes the mode of each lower left point, upper right, and midpoint. The mode slip line was also close to the experimental result.

The statistical hypothesis testing showed that the probability distribution of most of the failure timings had a normal distribution, although one of failure region displayed a log-normal distribution. The data from 0.22 to 0.24 in Fig. 7 were excluded in the later Smirnov–Grubbs testing; their mode and mean were also close to the experimental results.

For example, the seventh model in the numerical simulation had the result that was the closest to the experimental results. Figure 10 and Figure 11 show the horizontal acceleration wave at the center of slope crest and on top of the slope in experiment and numerical analysis, respectively. In this case, the horizontal distance from top of slope and the point of failure at stage 11 were about 6.0×10^{-2} m. There was little difference between the experimental and numerical analysis about the phase of the acceleration response at the center of the slope crest located away from the failure area. The absolute value of the acceleration in the numerical simulation was smaller than that in the experimental analysis because the porosity decreases and particles were constrained when they assemble because of the larger particle size compared to the experimental in the former. On the other hand, there was a phase shift accompanying the failure in experiment and simulation. This was because the acceleration meter was lifted up with the failure of the slope and measured a factor which was not the horizontal acceleration in the experiment.

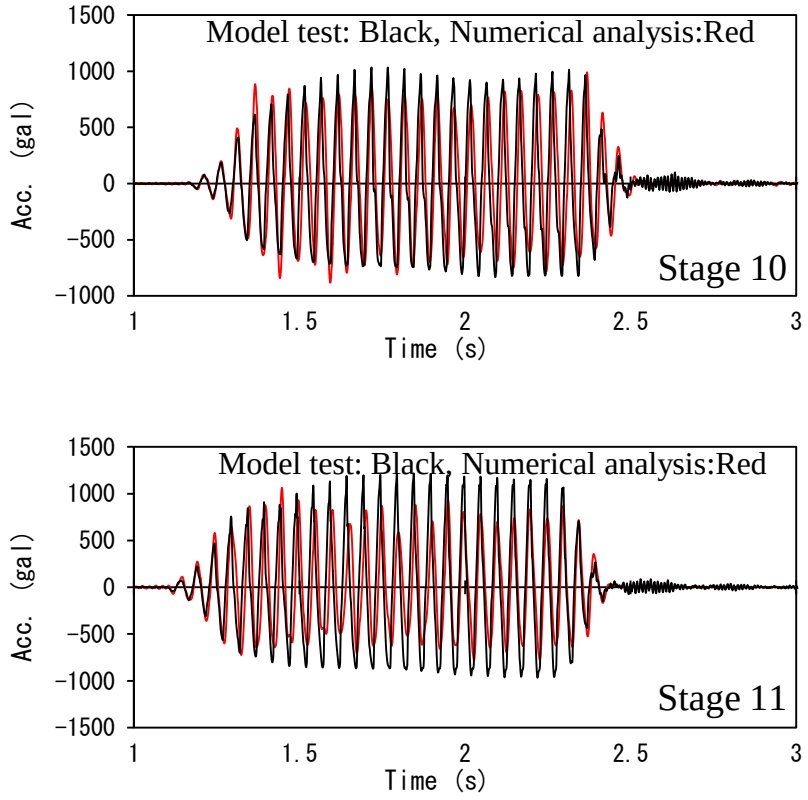

Figure 10. The horizontal acceleration wave at the center of the slope crest

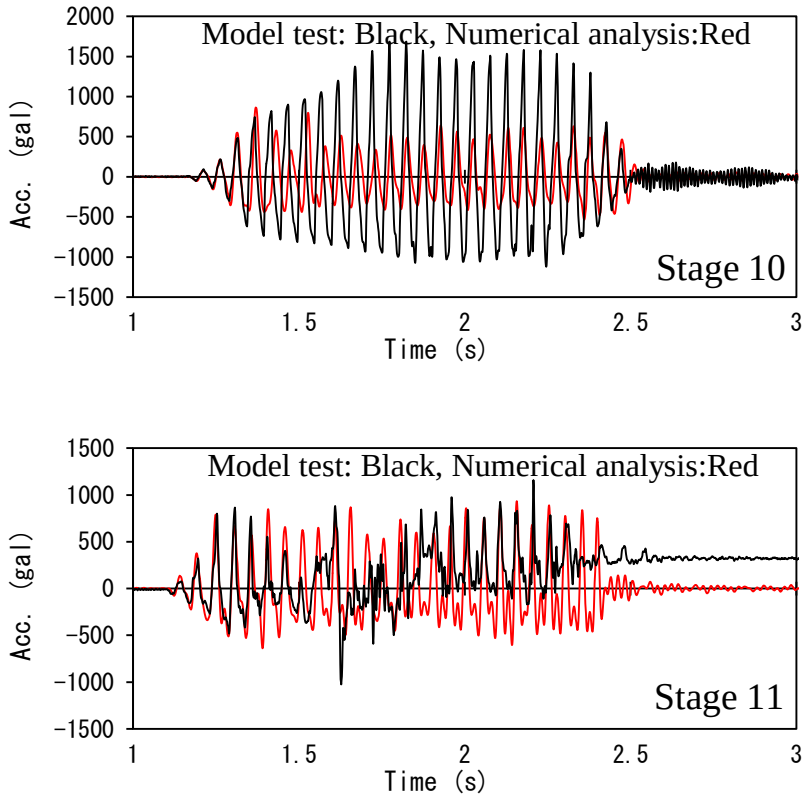

Figure11. The horizontal acceleration wave at the top of the slope

Based on these analysis results, the EDEM is so effective for a highly developed PRA because a stability analysis can be performed before a slope failure, and there is realistic information on the failure area when some analytical methods are not used, in contrast to the distinction between a stability analysis using the FEM and a failure analysis using the DEM. An example of realistic information is the velocity of the particles at the moment the slope failures. Analytical cases using by the EDEM like this can also narrow down the calculations of the probability distribution of impact force on the reactor building wall and evaluating the probability distribution of it reaching reactor building.

4.2. The next deployment for highly developed seismic probabilistic risk assessment

If there is the possibility of a critical effect on structures near the slope from rock movement although the frequency of this is low, and it is decided that this cannot be ignored as in Figure 1, Equation (3) below, based on the sequence of events from slope failure as presented in Figure 12 [1], is needed to evaluate risk:

$$P_{f\_ijkl} = P_{0i} \times P_{1j} \times P_{2k} \times P_{3l} \tag{3}$$

where P_{0i} stands for the exceedance probability of the peak ground acceleration i of the earthquake, P_{1j} denotes the probability of occurrence of scenario j of slope failure, P_{2k} signifies the probability of rock movement reaching reactor building, and P_{3l} the probability of falling rocks causing a failure in the reactor building.

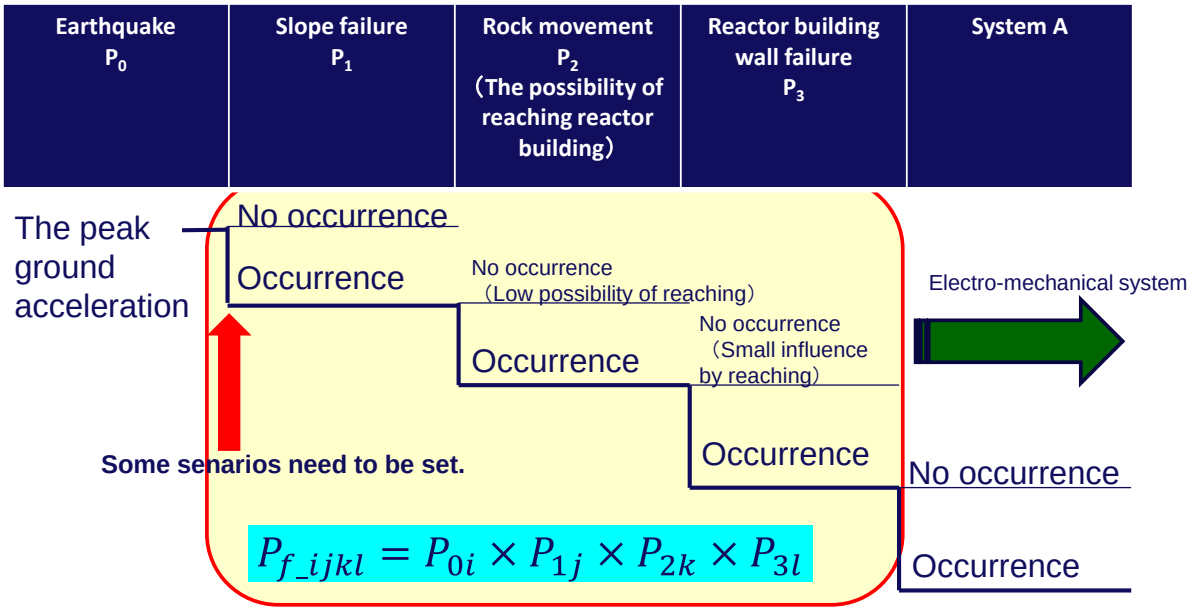

Figure12. The sequence of events from slope failure [1]

From the analytical results calculated by the EDEM and explained in this section, it can be concluded that P_{1j} and P_{2k} can be calculated as rational approaches, compared to the current methodology, that do not have an excessively conservative margin for the results. It is important to exclude the excessively conservative margin and evaluate the different phenomena accurately; this is important because seismic risk evaluation involves the evaluation of many successive phenomena.

5. CONCLUSION

This research investigated the applicability of DE analysis to analyse the earthquake response of a slope and the statistical patterns therein. The probability distribution of the failure timing was found to match normal distribution, although one failure region showed log-normal distribution. Their mode and mean were close to experimental results. So experimental result may be interpreted based on the statistical analysis by the initial particle arrangements given that strength-deformation parameters are fixed in EDEM.

The next step will be to evaluate the seismic failure probability of the reactor building with a highly developed PRA, firstly to calculate the probability distribution of impact force on reactor building wall. An experiment also will be needed to validate the corresponding impact force.

References

[1] Nakajima, M., Tochigi, H., Ozawa, K., Nomura, Y. "*Development of seismic risk assessment of rock slope*", (submitted to *Proc. Annu. Conf. JSCE*), (2018). (in Japanese)
[2] Ishimaru, M., Okada, T., Nakamura, H., Kawai, T., Kazama, M. "*Modelling of strength and deformation characteristics after shear failure of soft rock and application to evaluation of seismic stability of slopes against sliding*", J. Jpn. Soc. Civil Eng. Ser. C, 73(1), pp. 23-38, (2017). (in Japanese)
[3] Cundall, P.A., Strack, O.D.L. "*A discrete numerical model for granular assemblies*", Geotechnique, 29(1), pp. 47-65, 1979.
[4] Tochigi, H., Nomura, Y., Ozawa, K. "*DEM analysis of falling rocks' reaching distance providing that surrounding slope in nuclear power plant facility failures*", (submitted to *Proc. Annu. Conf JSCE*), (2018). (in Japanese)
[5] Hakuno, M. "*Simulation of rupture-tracing rupture by an extended distinct element method*", Tokyo: Morikita Publishing Co., Ltd., 1997.
[6] O'Sullivan, C. "*Particulate Discrete Element Modelling: A Geo-mechanics Perspective*", New York: Taylor & Francis Group, 2011.
[7] Yoshida, T., Tochigi, H. "*Numerical Simulation on Inclining Model Experiment by Extended Distinct Element Method*", *Proceedings of the 52nd Japan National Conference on Geotechnical Engineering*, 0861, pp. 1719-1720, (2017). (in Japanese)
[8] Yoshida, I. "*Basic study on failure analysis with using MPS method*", J. Jpn. Soc. Civil Eng. Ser. C, 73(1), pp. 93-104, (2011). (in Japanese)